Lectures on Random Matrices (Spring 2025)
Lecture 12: Random Growth Models

Leonid Petrov

Wednesday, April 2, 2025*

Contents

*Course webpage • Live simulations • TeX Source • Updated at 13:31, Wednesday 2nd April, 2025

1 Recap

In our last lecture, we explored the asymptotics of Dyson Brownian Motion with an outlier. We specifically focused on the phase transition that occurs when a rank-1 perturbation is applied to a random matrix ensemble.

1.1 Dyson Brownian Motion with Determinantal Structure

We established that for $\beta = 2$, the eigenvalues of the time-evolved process form a determinantal point process. The transition probability from an initial configuration $\mathbf{a} = (a_1 \geq \cdots \geq a_N)$ to a configuration $\mathbf{x} = (x_1 \geq \cdots \geq x_N)$ at time t is given by:

$$P(\lambda(t) = \mathbf{x} \mid \lambda(0) = \mathbf{a}) = N! \Big(\frac{1}{\sqrt{2\pi t}}\Big)^N \prod_{1 \leq i < j \leq N} \frac{x_i - x_j}{a_i - a_j} \det\Big[\exp\Big(-\frac{(x_i - a_j)^2}{2t}\Big)\Big]_{i,j=1}^N$$

This determinantal structure enabled us to derive the correlation kernel:

$$K_t(x, y) = \frac{1}{(2\pi)^2 t} \int \int \exp\Big(\frac{w^2 - 2yw}{2t}\Big) \Big/ \exp\Big(\frac{z^2 - 2xz}{2t}\Big) \prod_{i=1}^n \frac{w - a_i}{z - a_i} \frac{dw\, dz}{w - z} \tag{1.1}$$

where the contours of integration are specified to maintain analytical properties.

1.2 The BBP Phase Transition

The central focus was the Baik-Ben Arous-Péché (BBP) phase transition that occurs with finite-rank perturbations of GUE matrices. For the rank-1 case, we analyzed:

$$A + \sqrt{t}G, \quad \text{where } A = \operatorname{diag}(a\sqrt{n}, 0, \ldots, 0)$$

Through asymptotic analysis using steepest descent methods, we identified three distinct regimes:

1. **Airy regime** ($a < 1$): The largest eigenvalue follows the Tracy-Widom GUE distribution, just as in the unperturbed case. The spike is too weak to escape the bulk.

2. **Critical regime** ($a = 1$): A transitional behavior occurs when $a = 1 + An^{-1/3}$, leading to a deformed Airy kernel:

$$\tilde{K}_{\text{Airy}}(\xi, \eta) = \frac{1}{(2\pi i)^2} \iint \frac{\exp\left\{\frac{W^3}{3} - \xi W - \frac{Z^3}{3} + \eta Z\right\}}{W - Z} \frac{W - A}{Z - A} dW\, dZ$$

3. **Gaussian regime** ($a > 1$): The largest eigenvalue separates from the bulk, becoming an "outlier" centered at $a + 1/a$. Its fluctuations follow a Gaussian distribution rather than the Tracy-Widom law.

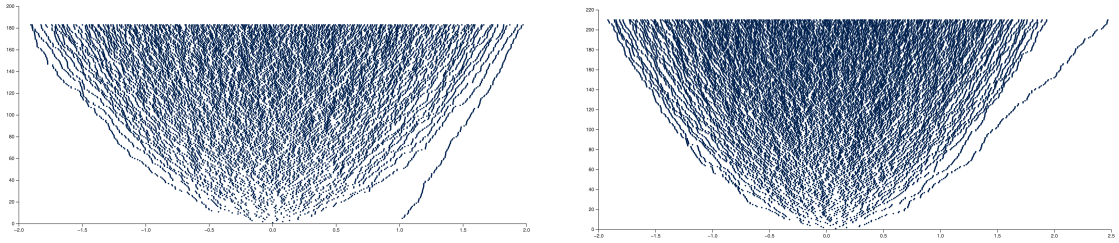

Figure 1: Two versions of the corners process with an outlier. Left: Corners process of $G + D$, where D is a rank-1 critical perturbation with eigenvalue 1. Right: Corners process of $G+UDU^\dagger$, where $U \in U(n)$ is a Haar-distributed unitary matrix and D is a rank-1 supercritical perturbation with eigenvalue 2 (the eigenvalue 1 is not visible in the rotated system). In both pictures, $n \approx 200$. See https://lpetrov.cc/simulations/2025-03-27-orthogonal-corners-outliers/ for an interactive simulation.

1.3 Remark: Corners process with outliers

One can also perturb the corners process structure, and get correlation kernels similar to (1.1) which we had for the Dyson Brownian Motion. The perturbed corners process is considered in [FF14], see also the earlier work [Met13] for the corners process of $UDU^\dagger$, where D is arbitrary and U is Haar-distributed. Both the kernels for the Dyson Brownian Motion and the corners process with outliers can be obtained from the formula of [Met13]. See Figure 1 for an illustration of the corners process with an outlier in two cases, when the basis for the outlier is rotated or not (the rotation does not affect the top level eigenvalue distribution, but has a significant effect on the whole corners process).

1.4 Goal today

Today, the goal is to survey various objects which arise in the KPZ universality class:

- The Airy line ensemble, which is the universal edge scaling limit of Dyson Brownian Motion, the corners process, and numerous statistical physics models.
- Moreover, the Airy line ensemble arises and is fundamental for a class of random growth models in one space and one time dimensions, which is known as the KPZ universality class.
- We will briefly mention how the Gaussian Free Field (GFF) arises in the KPZ class models in two space dimensions.
- We continue to discuss one particular model in the KPZ universality class — the Polynuclear Growth (PNG) and the related Last Passage Percolation (LPP) models.

2 A window into universality: Airy line ensemble

The edge scaling limit of Dyson Brownian Motion and the corners process[1] is a universal object for $\beta = 2$ models and determinantal structures (and far beyond). GUE formulas provide us with a powerful lens through which to examine these universality phenomena. In this section, we discuss the limiting behavior of Dyson Brownian Motion near the spectral edge, highlighting two of its fundamental properties: Brownian Gibbs property and characterization.

Theorem 2.1 (Edge scaling limit to Airy line ensemble)**.** *Consider an $N \times N$ GUE (Gaussian Unitary Ensemble) Dyson Brownian motion, i.e., the stochastic process of eigenvalues $(\lambda_1(t) \geq \cdots \geq \lambda_N(t))_{t\in\mathbb{R}}$ evolving under Dyson's eigenvalue dynamics. After centering at the spectral edge parallel to the vector $\mathbf{v}_t$ and applying the Airy scaling (tangent axis scaled by $N^{-1/3}$ and fluctuations scaled by $N^{-1/6}$), the top k eigenvalue trajectories converge as $N \to \infty$ to the **Airy line ensemble**. In particular, for each fixed $k \geq 1$ the rescaled process*

$$(N^{1/6}[\lambda_i(\langle N^{-1/3}, N^{-1/6}\rangle \cdot \mathbf{v}) - c_{N,t}])_{1\leq i\leq k}$$

converges in distribution (uniformly on compact t-intervals) to $(\mathcal{P}_i(t))_{1\leq i\leq k}$, where $\{\mathcal{P}_i(t)\}_{i\geq 1}$ is the parabolic Airy line ensemble.

Remark 2.2. The random variable $\mathcal{P}_1(0)$ has the GUE Tracy-Widom distribution.

Theorem 2.3 (Airy line ensemble is Brownian Gibbsian [CH16])**.** *The parabolic Airy line ensemble $\{\mathcal{P}_i(t)\}_{i\geq 1}$ satisfies the **Brownian Gibbs property**. Namely, for any fixed index $k \geq 1$ and any finite time interval $[a, b]$, conditioning on the outside portions of the ensemble (i.e., $\{\mathcal{P}_j(t) : t \notin [a, b]\}$ for all j, and $\{\mathcal{P}_j(t) : j \neq k\}$ for $t \in [a, b]$), the conditional law of the kth curve on $[a, b]$ is that of a **Brownian bridge** from $(a, \mathcal{P}_k(a))$ to $(b, \mathcal{P}_k(b))$ **conditioned** to stay above the $(k + 1)$th curve and below the $(k - 1)$th curve on $[a, b]$. In particular, the Airy line ensemble is invariant under this resampling of a single curve by a conditioned Brownian bridge.*

Theorem 2.4 (Characterization of ALE [AH23])**.** *The parabolic Airy line ensemble is the **unique** Brownian Gibbs line ensemble satisfying a natural parabolic curvature condition on the top curve. More precisely, let $\boldsymbol{\mathcal{P}} = (\mathcal{P}_1, \mathcal{P}_2, \ldots)$ be any line ensemble that satisfies the Brownian Gibbs property. Suppose in addition that the top line $\mathcal{P}_1(t)$ **approaches a parabola** of curvature $1/\sqrt{2}$ at infinity. Then $\boldsymbol{\mathcal{L}}$ must coincide (in law) with the **parabolic Airy line ensemble**, up to an overall affine shift of the entire ensemble.*

Let us define $\mathcal{L}_i(t) = \mathcal{P}_i(t) + t^2$, and call $\mathcal{L}$ the Airy Line Ensemble (without the word "parabolic"). One can think that the parabola comes from the scaling window, which is of different proportions in the horizontal and vertical directions. The non-parabolic Airy line ensemble $\mathcal{L}$ is time-stationary, that is, its distribution is invariant under time shifts $t \mapsto t + c$.

[1] Both without outliers — the presence of critical outliers may add a few extra lines (wanderers) to the Airy line ensemble, and we will not consider this complication here.

3 KPZ universality class: Scaling and fluctuations

3.1 Universality of random growth

In the $(1+1)$-dimensional **KPZ universality class**, random growth models exhibit a distinctive scale of fluctuations fundamentally different from classical Gaussian behavior. Kardar, Parisi, and Zhang [KPZ86] predicted that such interfaces have *roughness exponent* $1/2$ and *growth exponent* $1/3$, meaning that if time is scaled by a factor T, then horizontal distances scale by $T^{2/3}$ and vertical height fluctuations scale by $T^{1/3}$ [Rem22], as $T \to \infty$. Equivalently, the interface height $h(t,x)$ (after subtracting its deterministic mean growth) satisfies the $1:2:3$ *scaling*:

$$t^{-1/3}\Big(h(t,\chi t^{2/3}) - \mathbb{E}[h(t,\chi t^{2/3})]\Big) \qquad \text{converges in law as } t \to \infty.$$

These exponents $2/3$ and $1/3$ are universal in one-dimensional growth with local randomness, distinguishing the KPZ class from, e.g., diffusive (Edwards–Wilkinson) interfaces. Intuitively, the interface develops random peaks of size $O(t^{1/3})$, and correlations spread over a spatial range $O(t^{2/3})$—a highly nontrivial, super-diffusive scaling.

3.2 KPZ equation

The KPZ equation is a continuous model of random growth which was first proposed non-rigorously in the physics literature [KPZ86], and then justified mathematically. There are several justifications, including the one by Hairer [Hai14]. The equation reads (ignoring the constant by the terms in the right-hand side):

$$\partial_t h(t,x) = \partial_{xx} h(t,x) + \big(\partial_x h(t,x)\big)^2 + \xi(t,x), \qquad t>0, \quad x \in \mathbb{R}, \tag{3.1}$$

where ξ is the space-time white noise, that is, a Gaussian process with

$$\mathbb{E}[\xi(t,x)\xi(t',x')] = \delta(t-t')\delta(x-x').$$

The terms in the KPZ equation stand for the three types of interactions driving the random growth process:

- The first term $\partial_{xx} h$ is a *smoothing* heat equation term, which is a classical diffusion (independent growth) term.
- The second term $\big(\partial_x h\big)^2$ is a *slope-dependent growth* term, which tends to close high-slope gaps. This mechanism is visible in discrete models which we will see in Section 4.
- The third term $\xi(t,x)$ is a *stochastic noise* term which favors independent growth at each location. This leads to roughening of the interface.

Note that the equation (3.1) is ill-posed even in the sense of distributions, since squaring a distribution $\partial_x h$ is not well-defined. Instead, to solve the KPZ equation in one space dimension $x \in \mathbb{R}$, one can formally write $h = \log Z$, where Z then solves the well-posed *stochastic heat equation* (SHE) with multiplicative noise:

$$\partial_t Z(t,x) = \partial_{xx} Z(t,x) + \xi(t,x) Z(t,x).$$

The stochastic heat equation is linear in Z, and there are no issues with defining the solution. The passage from h to $Z = \exp(h)$ is known as the *Cole-Hopf transformation*. It is not rigorous either, but was used prior to [Hai14] to define what it means to have a solution to (3.1).

3.3 First discoveries

One of the most striking discoveries is that the **one-point distribution** of these fluctuations, when the growth starts from the so-called *droplet* (or *narrow wedge*) initial condition, is governed by the GUE *Tracy–Widom law*, rather than a normal law. The **Tracy–Widom distribution** (for Gaussian Unitary Ensemble, GUE) describes the fluctuations of the largest eigenvalue of a random Hermitian matrix. In the KPZ class, the same distribution emerges in the long-time limit for a wide range of models and initial conditions. For example, in the Totally Asymmetric Simple Exclusion Process (TASEP) with step initial data (corresponding to the narrow wedge), the height at the origin, when centered and scaled by $t^{1/3}$, converges in law to the Tracy–Widom GUE distribution [Joh00], [Rem22]. This was the first rigorous confirmation of $1/3$ fluctuations in a random growth model. Such behavior is believed to be *universal*: many other integrable models (polynuclear growth, last-passage percolation, directed polymers, etc.) exhibit the same long-time distribution and scaling exponents.

In the next Section 4, we will discuss a particular semi-discrete random growth model — the Polynuclear Growth (PNG).

3.4 Effect of initial conditions

Crucially, the exact form of the limiting distribution depends on the *initial condition* of the growth process. Different symmetry classes of random matrices appear:

- **Curved (droplet) initial data:** Starting from a narrow peak (often called *narrow wedge* or droplet initial condition), the height fluctuations follow the Tracy–Widom GUE distribution in the $t \to \infty$ limit. This corresponds to the *unitary* symmetry class (e.g. complex Hermitian matrices).
- **Flat initial data:** Starting from a flat interface (e.g. all zero initial height), fluctuations converge to the Tracy–Widom GOE distribution, which is the law of the largest eigenvalue of a random real symmetric (Gaussian orthogonal ensemble) matrices, with *orthogonal* symmetry.
- **Stationary initial data:** Starting from a two-sided Brownian or otherwise stationary initial profile, the fluctuation distribution is again non-Gaussian but neither GOE nor GUE. In this case one obtains the *Baik–Rains distribution*, often denoted F_0, which was first derived by Baik and Rains for a stationary last passage percolation model [BR00].

3.5 Remark: Gaussian Free Field in KPZ universality

The KPZ equation (3.1) can be posed in any space dimension:

$$\partial_t h(t,x) = Dh(t,x) + (\nabla h(t,x))^2 + \xi(t,x), \qquad t > 0, \quad x \in \mathbb{R}^d,$$

where D is a second-order differential operator, and ∇ is the gradient. In $d = 2$ case, the operator D can have one of the two signatures:

$$D = \Delta \quad \text{or} \quad D = \partial_x^2 - \partial_y^2.$$

These two cases are known as *isotropic* and *anisotropic* KPZ equations, respectively.

The isotropic KPZ equation is much more mysterious than the anisotropic one. In the anisotropic case, it is believed that the fluctuations scale with exponent 0 (as opposed to 1/3 for one dimension), while in the isotropic case, even the hypothetical fluctuation scaling exponent is debated.

Further evidence for the anisotropic case is the existence of exactly solvable growth models in this class (e.g., [BF14]), which have logarithmic fluctuations. Moreover, their fluctuations are governed by the Gaussian Free Field (GFF), which we encountered earlier in Lecture 9. Moreover, the GFF should be the stationary distribution for the anisotropic KPZ fixed point (Markov process which should be the long-time scaling limit of the anisotropic KPZ equation).

Back to random matrices, consider the following question:

> Can we imagine a 2-dimensional random growth model on random matrices, which will look like the 2-dimensional anisotropic KPZ equation? It would have random growth features, where some 2-dimensional surface is growing, and will have the GFF fluctuations.

We know an object in random matrices with GFF fluctuations — the height function of the corners process. So, a natural guess is to take the Brownian motion on matrix elements, and look at the evolution of the corners eigenvalues. However, the evolution of the eigenvalues of all corners is *not* going to be Markov. A workaround is the construction by Warren [War07], which produces the relevant Markov process on the full interlacing corners configuration.

4 Polynuclear Growth and Last Passage Percolation

4.1 Definition and single-layer PNG

We start with the *single-layer* PNG model on the real line. The interface height $h(t, x)$ evolves in continuous time $t \geq 0$ over the spatial coordinate $x \in \mathbb{R}$ and has piecewise-constant plateaus with sharp upward steps. In other words, $h(t, x)$ is piecewise constant in x, and takes integer values.

Dynamics. The evolution is described by two basic ingredients:

1. *Nucleation events:* At random times and locations (t, x) in the plane, a new "island" of height 1 is born atop the existing surface. Each newly born island sits just above $h(t, x)$, creating a step of height 1 at the precise point x and time t. We assume that the nucleation events form a Poisson process in space-time (t, x).

2. *Lateral spread:* Once an island is created at height $k + 1$, its boundaries spread outward (to the left and right in x) with speed 1. Thus a step boundary moves in both directions until it merges with another step boundary or nucleation event. When the islands merge, the height becomes flat at this point.

See Figure 2 for an illustration of the single-layer PNG model. See also Figure 3 for an evolution of the nucleation events, each of which spreads at speed 1.

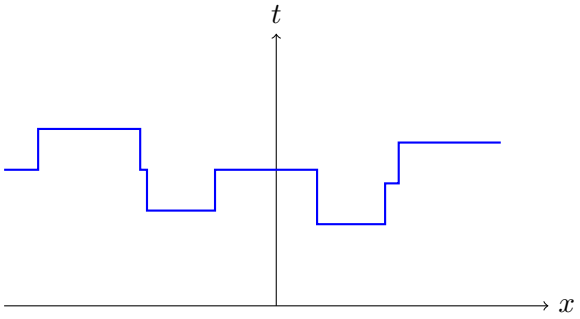

Figure 2: Polynuclear Growth (PNG) model interface.

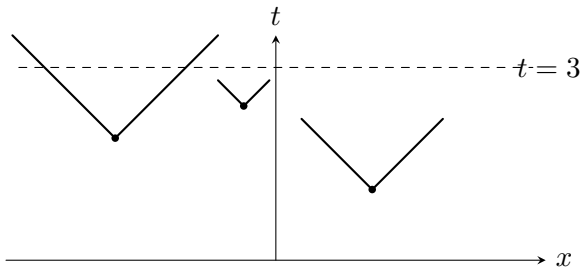

Figure 3: Single-layer PNG: Nucleations (black dots) appear randomly in the (t, x) plane according to a Poisson process. Each nucleation creates an upward step of height 1. The boundary of each newly created island expands laterally at speed 1.

Initialization. One typically imposes an initial condition $h(0, x)$ on the spatial axis (e.g., a single spike or droplet, or a flat interface). The flat interface is $h(0, x) = 0$ for all $x \in \mathbb{R}$, and the droplet is a single upward step at $x = 0$ with height 1. In the droplet case, we also set $h(0, x) = -\infty$ for $x \neq 0$, for convenience.

4.2 Multiline PNG

The *multiline* version of PNG tracks multiple height levels by stacking interfaces at multiple layers, $h_k(t, x)$. A merging event at layer k produces a nucleation event at layer $k + 1$. So, the nucleation at h_1 is powered by the Poisson process, while the nucleation at each h_k, $k \geq 2$, is powered by the merges at h_{k-1}. The initial condition is assumed to satisfy

$$h_1(0, x) \geq h_2(0, x) \geq \cdots, \qquad \text{for all } x \in \mathbb{R}.$$

This ordering is preserved by the evolution, see Problem L.1.

We see that the evolution of $h_2, h_3, \ldots$ is just a function of the full space-time evolution of h_1. However, at fixed time t, the functions $h_k(t, \cdot)$ cannot be determined just by $h_1(t, \cdot)$.

The evolution of all the h_k's can be modeled on the same Poisson process plot, by looking at "shadow lines", the lines of the second, third, etc. orders arising when two lines of the previous order merge.

4.3 KPZ mechanisms in the PNG growth

Let us compare the single-layer PNG growth with the ingredients of the KPZ equation (3.1):

- Independent nucleation events in the PNG model correspond to the stochastic noise term $\xi(t,x)$ in the KPZ equation.
- The lateral spread of step boundaries in PNG is akin to the slope-dependent growth term $(\partial_x h)^2$ in KPZ. Indeed, if the slope is large, the growth at a given point happens with higher speed.
- The diffusion smoothing mechanism is not quite visible, but one can think of it as the effect of the nucleation events, which are spread out in space and time.

4.4 Last Passage Percolation (LPP)

Let us now describe the height function $h_1(t,x)$ of the top layer of the PNG model as a percolation problem in the Poisson environment. Consider a Cartesian coordinate system with axes u and v. Let t represent the diagonal "time" axis, defined as $t = u + v$. Now, imagine a Poisson point process $\mathcal{P}$ of intensity 1 in the upper half-plane $\{(u,v) : u \geq 0, v \geq 0\}$. For two points (u_1, v_1) and (u_2, v_2) with $u_1 \leq u_2$ and $v_1 \leq v_2$, an up-right path from (u_1, v_1) to (u_2, v_2) is a continuous curve moves only rightward (increasing u) or upward (increasing v). The weight of a path is defined as the number of Poisson points it collects along the way.

The last passage time $\mathcal{P}[(u_1, v_1) \to (u_2, v_2)]$ is defined as the maximum weight among all up-right paths from (u_1, v_1) to (u_2, v_2):

$$\mathcal{P}[(u_1, v_1) \to (u_2, v_2)] = \max_{\pi:(u_1,v_1)\to(u_2,v_2)} \#\{\text{Poisson points collected by } \pi\}$$

This maximum is always attained by some piecewise linear path and represents a random variable that depends on the Poisson environment $\mathcal{P}$.

Proposition 4.1. *For the PNG model with the droplet initial condition, the height function $h_1(t,x)$ at position x and time t can be expressed as:*

$$h_1(t,x) = \mathcal{P}[(0,0) \to (u,v)]$$

where the coordinates (u,v) satisfy $u + v = t$ and $u - v = x$. In other words, the point (u,v) lies on the diagonal "time" line $t = u + v$ at the spatial position corresponding to $x = u - v$.

Proof. See Problem L.2. □

4.5 Topics to continue

- Multipath LPP and multi-layer PNG: $h_1 + \ldots + h_k$ (with the droplet initial condition) has the same distribution as $\mathcal{P}^{(k)}[(0,0) \to (t+x, t-x)]$, the k-path point-to-point LPP distribution.
- Connection to the Airy line ensemble — PNG with the droplet initial condition converges to the Airy line ensemble. (Same it true of the LPP, by the mapping.) So, the PNG/LPP with the droplet initial condition is related to Hermitian symmetric random matrices.
- PNG with flat initial condition / LPP in the point-to line regime converge to the GOE Tracy-Widom distribution. This initial condition is somehow related to real symmetric random matrices.
- The full scaling limit — the flat initial condition version of the Airy line ensemble — is less understood. In particular, its Gibbs property is not quite clear.
- Multipoint PNG fluctuations are asymptotically described by the KPZ fixed point Markov process [MQR21], and, in full generality of fluctuations, by an object known as Directed Landscape [DOV22].
- Possible next item to explore: Mapping LPP to the Wishart-Laguerre ensemble.

L Problems (due 2025-04-29)

L.1 PNG ordering

If the initial conditions at time 0 of the multiline PNG satisfy

$$h_1(0,x) \geq h_2(0,x) \geq \cdots, \qquad \text{for all } x \in \mathbb{R},$$

then show that they continue to satisfy the same ordering at all times $t > 0$.

L.2 PNG and last passage percolation

Prove Proposition 4.1.

References

[AH23] A. Aggarwal and J. Huang, *Strong Characterization for the Airy Line Ensemble*, arXiv preprint (2023). arXiv:2308.11908. ↑4

[BF14] A. Borodin and P. Ferrari, *Anisotropic growth of random surfaces in 2+1 dimensions*, Commun. Math. Phys. **325** (2014), 603–684. arXiv:0804.3035 [math-ph]. ↑7

[BR00] J. Baik and E. Rains, *Limiting distributions for a polynuclear growth model with external sources*, Jour. Stat. Phys. **100** (2000), no. 3, 523–541. arXiv:math/0003130 [math.PR]. ↑6

[CH16] I. Corwin and A. Hammond, *KPZ line ensemble*, Probability Theory and Related Fields **166** (2016), no. 1-2, 67–185. arXiv:1312.2600 [math.PR]. ↑4

[DOV22] D. Dauvergne, J. Ortmann, and B. Virág, *The directed landscape*, Acta Math. **229** (2022), 201–285. arXiv:1812.00309 [math.PR]. ↑10

[FF14] P. Ferrari and R. Frings, *Perturbed GUE minor process and Warren's process with drifts*, J. Stat. Phys **154** (2014), no. 1-2, 356–377. arXiv:1212.5534 [math-ph]. ↑3

[Hai14] M. Hairer, *Solving the KPZ equation*, Ann. Math. (2) **178** (2014), no. 2, 559–664. arXiv:1109.6811 [math.PR]. ↑5, 6

[Joh00] K. Johansson, *Shape fluctuations and random matrices*, Commun. Math. Phys. **209** (2000), no. 2, 437–476. arXiv:math/9903134 [math.CO]. ↑6

[KPZ86] M. Kardar, G. Parisi, and Y. Zhang, *Dynamic scaling of growing interfaces*, Physical Review Letters **56** (1986), no. 9, 889. ↑5

[Met13] A. Metcalfe, *Universality properties of Gelfand-Tsetlin patterns*, Probab. Theory Relat. Fields **155** (2013), no. 1-2, 303–346. arXiv:1105.1272 [math.PR]. ↑3

[MQR21] K. Matetski, J. Quastel, and D. Remenik, *The KPZ fixed point*, Acta Math. **227** (2021), no. 1, 115–203. arXiv:1701.00018 [math.PR]. ↑10

[Rem22] D. Remenik, *Integrable fluctuations in the KPZ universality class*, Proc. Int. Congr. Math. 2022 (2022), 4426–4450. arXiv:2205.01433 [math.PR]. ↑5, 6

[War07] J. Warren, *Dyson's Brownian motions, intertwining and interlacing*, Electron. J. Probab. **12** (2007), no. 19, 573–590. arXiv:math/0509720 [math.PR]. ↑7

L. Petrov, University of Virginia, Department of Mathematics, 141 Cabell Drive, Kerchof Hall, P.O. Box 400137, Charlottesville, VA 22904, USA

E-mail: lenia.petrov@gmail.com